Inorg. Chem. **2005**, *44*, 1263–1274

Experimental and Theoretical Studies of Carbodiphosphorane–CX_2 Adducts with Unusual Bonding Situations: Preparation, Crystal Structures, and Bonding Analyses of $S_2CC(PPh_3)_2$, $O_2CC(PPh_3)_2$, and $[(CO)_4MS_2CC(PPh_3)_2]$ (M = Cr, Mo, W)†

Wolfgang Petz,* Christian Kutschera, Maya Heitbaum, Gernot Frenking,* Ralf Tonner, and Bernhard Neumüller*

Fachbereich Chemie, Philipps-Universität Marburg, Hans-Meerwein-Strasse, D-35032 Marburg, Germany

Received November 15, 2004

We report about the first X-ray structure analyses of the CS_2 and CO_2 adducts with carbodiphosphorane $C(PPh_3)_2$ and the synthesis and X-ray structure analysis of group 6 carbonyl complexes with compound $S_2CC(PPh_3)_2$ as a ligand $[(CO)_4MS_2CC(PPh_3)_2]$ (M = Cr, Mo, W). The nature of the carbon–carbon bonding in $X_2CC(PPh_3)_2$ and in the model compounds $X_2CC(PH_3)_2$ and the metal–ligand bonding in $[(CO)_4MoS_2CC(PH_3)_2]$ have been analyzed with charge and energy decomposition methods using DFT calculations. Carbodiphosphoranes $C(PR_3)_2$ are double electron pair donors having σ- and π-carbon lone-pair orbitals as the two highest occupied MOs.

Introduction

The linear 16-electron species CX_2 (X = O, S), which have electrophilic carbon atoms, can be activated by various donors D forming adducts with approximate sp^2 hybridization at carbon. Under special electronic conditions CX_2 can be fixed at transition metals in an η^2(C,X) coordination mode (X = O;[1] X = S)[2] via the p(π) orbitals, which mimics the coordination chemistry of olefines. Furthermore, CS_2 bonded to a transition metal in such a manner is the main source for the preparation of transition metal thiocarbonyl complexes.[3]

As depicted in Scheme 1, addition compounds between CS_2 and neutral donor molecules D are known with phosphines (**I**), carbenes (**II**), ylides (**III**), and carbodiphosphoranes (**IV**). In the adducts **II** to **IV** carbon−carbon bonds are formed. While the adducts of the type **I** mainly with tricyclohexyl- or trimethylphosphine have developed a rich chemistry,[4] to our knowledge, only two examples of **II** are described with electron rich carbene compounds[5−7] and the chemistry is restricted to only a few reactions. Similarly, some adducts with ylides (**III**) such as $S_2CC(Me_2)PPh_3$ are also known[8] along with anionic species $[S_2CC(R)P(NMe_2)_3]^-$.[9] Concerning the compounds of the type **IV**, only the adduct with $Ph_3P{=}C{=}PPh_3$ (**1**) is described as the sparingly soluble

Scheme 1

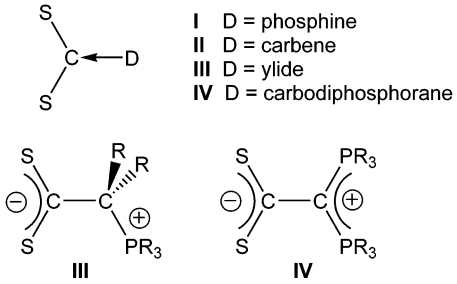

† This paper is dedicated to Professor Paul v. R. Schleyer on the occasion of his 75th birthday.

* Authors to whom correspondence should be addressed. E-mail: petz@staff.uni-marburg.de (W.G.); frenking@chemie.uni-marburg.de (G.F.). neumuell@chemie.uni-marburg.de (B.N.).

(1) (a) Walther, D. *Coord. Chem. Rev.* **1987**, *79*, 135. (b) Behr, A. *Angew. Chem.* **1988**, *100*, 681. Behr, A. *Angew. Chem., Int. Ed. Engl*. **1988**, *27*. 661. (c) Hirano, M.; Akita, M.; Tani, K.; Kumagai, K.; Kasuga, N. C.; Fukuoka, A.; Komiya, S. *Organometallics* **1997**, *16*, 4206 and literature therein.

(2) Bianchini, C.; Mealli, C.; Meli, A.; Sabat, M. In *Stereochemistry of Organometallic and Inorganic Compounds*, Bernal, I., Ed.; Elsevier: Amsterdam, 1986; Vol. 1, p 146.

(3) Broadhurst, P. V. *Polyhedron* **1985**, *4*, 1801.

(4) See for example: (a) Bianchini, C.; Ghilardi, C. A.; Meli, A.; Midollini, S.; Orlandini, A. *Organometallics* **1982**, *1*, 778. (b) Galindo, A.; Mealli, C. *Inorg. Chem.* **1996**, *35*, 2406. (c) Lopez, E. M.; Miguel, D.; Perez, J.; Riera, V.; Bois, C.; Jeannin, Y. *Organometallics* **1999**, *18*, 490 and references therein. For substituted phosphines, see: (d) Petz, W.; Weller, F. *J. Chem. Soc., Chem. Commun.* **1995**, 1049. (e) Yih, K.-H.; Lin, Y.-C.; Cheng, M. C.; Wang, Y. *J. Chem. Soc., Chem. Commun*. **1993**, 1380.

(5) Kuhn, N.; Bohnen, H.; Henkel, G. *Z. Naturforsch*. **1994**, *49b*, 1473.

(6) Ziegler, M. L.; Weber, H.; Nuber, B.; Serhadle, O. *Z. Naturforsch*. **1987**, *42b*, 1411.

(7) Kuhn, N.; Weyers, G.; Henkel, G. *J. Chem. Soc., Chem. Commun*. **1997**, 627.

10.1021/ic048397l CCC: $30.25
Published on Web 02/05/2005

bright yellow orange compound $S_2CC(PPh_3)_2$ (**2**), which serves as a precursor for the preparation of the heterocumulene S═C═C═PPh_3 with loss of $SPPh_3$.[10] Related adducts (also called "inner salts") of **1** with CO_2 and COS[10] as well as with the carbon dioxide-like heteroallene PhN═C═NPh[11,12] are also known, but a geometry determination of **2** through X-ray structure analysis was not possible until now. Adducts of **1** with other Lewis acids were described resulting in carbon bonds to main group elements[13] or transition metals[14] and confirmed by crystal structures; the coordination chemistry of ylides up to 1996 has been reviewed.[15]

In general the CS_2 adducts **I** to **IV** are capable of forming transition metal complexes with sulfur-to-metal bonds, and compounds of this type are important in biochemical processes because sulfur donors have found to surround the metal atoms of many metalloenzymes mainly containing Mo and Fe as central atoms.[16] While derivatives of **I**−**III** are known to act as monodentate or chelating complex ligands, similar to the negatively charged dithiocarbaminates,[17] nothing is reported about the ligand behavior of the type **IV** compound $S_2CC(PPh_3)_2$ (**2**).

There are two major differences between the ylidic adducts **III** and **IV**. One feature is the hybridization at the donor carbon atom, being sp^3 at the ylide and sp^2 at the carbodiphosphorane. The second major difference is the distribution of the positive charge, which in **III** is located at the phosphorus atom while in **IV** the charge is allowed to spread over three atoms including the carbon atom. These facts promised new and unusual properties and prompted us to study the crystal structures of the adducts $S_2CC(PPh_3)_2$ (**2**) and $O_2CC(PPh_3)_2$ (**3**) and the behavior of **2** as a potential complex ligand toward various transition metals.

Scheme 2

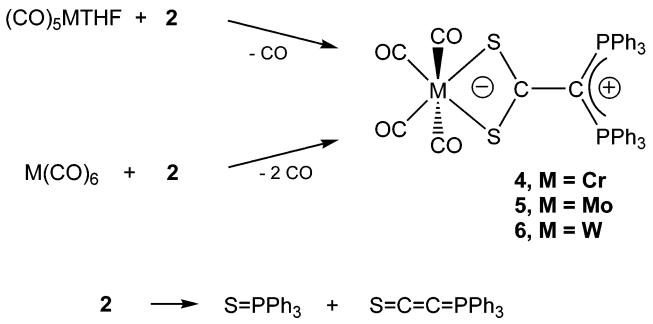

In this contribution we describe the crystal structure of the zwitterionic compounds $S_2CC(PPh_3)_2$ (**2**) and $O_2CC(PPh_3)_2$ (**3**) and the syntheses and the crystal structures of group 6 transition metal carbonyl complexes containing **2** as ligand. The unusual bonding situations in **2**, **3**, and in the metal complexes are studied by quantum theoretical calculations.

Results and Discussion

The CS_2 adduct **2** is obtained as a bright orange precipitate by addition of an excess CS_2 to a toluene solution of **1** at room temperature. The colorless CO_2 adduct **3** is similarly formed as a precipitate by bubbling CO_2, which was dried over P_2O_5 through a toluene solution of **1** following the procedure described earlier.[10] Both compounds are insoluble in THF, toluene, and other hydrocarbons.

If the photochemically generated adducts $[(CO)_5MTHF]$ were allowed to react with **2** at room temperature, the novel complexes $[(CO)_4MS_2CC(PPh_3)_2]$ (**4**, M = Cr; **5** M = Mo; **6** M = W) were obtained in moderate yields as red orange crystals (Scheme 2). Under these conditions the formation of small amounts of $SPPh_3$ and the heterocumulene S═C═C═PPh_3 were detected by ^{31}P NMR spectroscopy as indicated by the signals at 42.3 and 10.3 ppm, respectively. This splitting was the only known reaction of **2** since the first preparation of this adduct. The complex **5** is also formed, when a suspension of the insoluble adduct **2** in THF is treated at room temperature for several days with $Mo(CO)_6$; during the reaction time the majority of **2** dissolves with formation of an orange solution. However, the ^{31}P NMR spectrum of this solution showed that the amounts of the byproducts mentioned above have increased relative to **5**. Under these conditions $Cr(CO)_6$ and $W(CO)_6$ produce only small amounts or traces of **4** and **6** and the byproducts $SPPh_3$ and S═C═C═PPh_3 dominate. The complexes **4**−**6** represent the first examples in which the neutral zwitterionic compound **2** serves as a ligand in transition metal chemistry and in all cases **2** acts as a chelating ligand.

The ^{31}P NMR spectrum of the THF solutions exhibit singlets at 8.9 (**4**), 14.7 (**5**) and 13.8 ppm (**6**). The chemical shifts do not differ markedly from those of related adducts of the carbodiphosphorane **1**. They all are shifted of about 10−25 ppm to lower field with respect to **1**.

The IR spectra of **4**−**6** are very similar and exhibit up to four strong bands in the CO region between 1800 and 2000 cm^{-1}, which indicate the presence of only terminal CO

(8) (a) Kunze, U.; Merkel, R. *J. Organomet. Chem.* **1981**, *219*, 69. (b) Uson, R.; Fornies, J.; Uson, M. A.; Mar Carranza, M. *Inorg. Chim. Acta* **1989**, *155*, 71.
(9) Petz, W.; Weller, F.; Schmock, F. *Z. Anorg. Allg. Chem.* **1998**, *624*, 1123.
(10) (a) Matthews, C. N.; Driscoll, J. S.; Birum, G. H. *J. Chem. Soc., Chem. Commun*. **1966**, 736. (b) Matthews, C. N.; Birum, G. H. *Tetrahedron Lett.* **1966**, *46*, 5707.
(11) (a) Ramirez, F.; Pilot, J. F.; Desai, N. B.; Smith, C. P.; Hansen, B.; McKelvie, N. *J. Am. Chem. Soc*. **1967**, *89*, 6273. (b) Ross, F. K.; Manojlovic-Muir, L.; Ramirez, F.; Pilot, J. F. *J. Am. Chem. Soc*. **1972**, *94*, 8738.
(12) Ross, F. K.; Hamilton, W. C.; Ramirez, F. *Acta Crystallogr*. **1971**, *27 B*, 2331.
(13) (a) Schmidbaur, H.; Zybill, C. E.; Neugebauer, D. *Angew. Chem*. **1982**, *94*, 321; *Angew. Chem., Int. Ed. Engl*. **1982**, *21*, 310. (b) Schmidbaur, H.; Zybill, C. E.; Neugebauer, D.; Müller, G. *Z. Naturforsch*. **1985**, *40b*, 1293. (c) Petz, W.; Kutschera, C.; Tschan, S.; Weller, F.; Neumüller, B. *Z. Anorg. Allg. Chem*. **2003**, *629*, 1235.
(14) (a) Petz, W.; Weller, F.; Uddin, J.; Frenking, G. *Organometallics* **1999**, *18*, 619. (b) Vicente, J.; Singhal, A. R.; Jones, P. G. *Organometallics* **2002**, *21*, 5887. (c) Sundermeyer, J.; Weber, K.; Peters, K.; von Schnering, H. G. *Organometallics* **1994**, *13*, 2560. (d) Zybill, C.; Müller, G. *Organometallics* **1987**, *6*, 2489. (e) Müller, G.; Krüger, C.; Zybill, C.; Schmidbaur, H. *Acta Crystallogr*. **1986**, *C42*, 1141.
(15) (a) Schmidbaur, H. *Angew. Chem.* **1983**, *95*, 980. Schmidbaur, H. *Angew. Chem., Int. Ed. Engl*. **1983**, *22*, 907. (b) Kaska, W. C. *Coord. Chem. Rev.* **1983**, *48*, 1. (b) Kolodiazhnyi, O. I. *Tetrahedron* **1996**, *52*, 1855. (c) Johnson, A. W. *Ylides and Imines of Phosphorus*; Wiley-Interscience Publication: New York, 1993.
(16) Sellmann, D. *Angew. Chem.* **1993**, *105*, 67. Sellmann, D. *Angew. Chem., Int. Ed. Engl.* **1993**, *32*, 64.
(17) (a) Willemse, J.; Cras, J. A.; Steggerda, J. J.; Keijzers, C. P. Structure and Bonding 28, Springer-Verlag: Berlin, 1976; 83. (b) Petz, W. *Z. Naturforsch.* **1976**, *31B*, 1007.

Table 1. Crystal Data and Structure Refinement Details for the Compounds **2**−**6**

	2	**3**	**4**	**5**	**6**
formula	$C_{38}H_{30}P_2S_2$	$C_{38}H_{30}O_2P_2$	$C_{50}H_{46}CrO_6P_2S_2$	$C_{50}H_{46}MoO_6P_2S_2$	$C_{44}H_{34}O_{4.5}P_2S_2W$
MW	612.72	560.60	920.97	964.92	944.67
crystal size (mm)	0.14 × 0.02 × 0.05	0.37 × 0.1 × 0.04	0.21 × 0.2 × 0.06	0.24 × 0.09 × 0.07	0.18 × 0.16 × 0.04
a (pm)	1275.2(2)	1193.9(1)	1049.3(1)	1052.8(1)	2139.4(1)
b (pm)	1461.7(3)	1705.3(1)	2230.2(3)	2229.4(2)	1738.5(1)
c (pm)	1626.6(3)	1510.9(1)	2050.5(2)	2050.5(2)	4238.4(2)
α (deg)	90	90	90	90	90
β (deg)	93.83(1)	102.86(1)	103.37(1)	102.82(1)	90
γ (deg)	90	90	90	90	90
volume (pm^3) × 10^6	3025(1)	2999.0(7)	4612.5(9)	4692.8(8)	15764(1)
Z	4	4	4	4	16
d_{calcd} (g/cm^3)	1.345	1.286	1.326	1.366	1.592
radiation	Mo Kα	Mo Kα	Mo Kα	Mo Kα	Mo Kα
abs correction (*μ*)	numeric (3.1 cm^{-1})	numeric (1.8 cm^{-1})	numeric (4.6 cm^{-1})	numeric (4.8 cm^{-1})	numeric (31.6 cm^{-1})
$2\theta_{max}$ (deg)	52.57	52.57	52.25	52.64	52.37
cryst syst	monoclinic	monoclinic	monoclinic	monoclinic	orthorombic
space group	*C*2/*c* (No. 15)	Cc (No. 9)	$P2_1/c$ (No. 14)	$P2_1/c$ (No. 14)	*Pbca* (No. 61)
diffractometer	IPDS II (Stoe)	IPDS II (Stoe)	IPDS I (Stoe)	IPDS II (Stoe)	IPDS II (Stoe)
temp (K)	193	193	193	193	193
index range	−15 ≥ h ≥ 15 −18 ≥ k ≥ 18 −20 ≥ l ≥ 20	−14 ≥ h ≥ 14 −21 ≥ k ≥ 21 −18 ≥ l ≥ 18	−13 ≥ h ≥ 12 −27 ≥ k ≥ 27 −23 ≥ l ≥ 23	−13 ≥ h ≥ 13 −27 ≥ k ≥ 26 −25 ≥ l ≥ 25	−26 ≥ h ≥ 24 −21 ≥ k ≥ 19 −50 ≥ l ≥ 50
no. of rflns collected	10797	21554	35628	33835	64728
no. of indep rflns (R_{int})	3047 (0.1105)	5793 (0.0787)	8758 (0.3601)	9433 (0.1192)	14754 (0.0869)
no. of obsd rflns ($F_0 > 4\sigma(F_0)$)	1925	4829	2721	4932	9531
params	192	380	408	516	965
H atoms	calcd positions with common displacement param	calcd positions with common displacement param	calcd positions with common displacement param	calcd positions with common displacement param	calcd positions with common displacement param
structure solution	Patterson-method; SHELXTL-Plus[20]	direct methods; SHELXS-97[21]	direct methods; Sir-92[23]	direct methods; SHELXS-97[21]	Patterson-method; SHELXTL-Plus[20]
refinement (F^2)	SHELXL-97[22]	SHELXL-97[22]	SHELXL-97[22]	SHELXL-97[22]	SHELXL-97[22]
Flack parameter		−0.03(7)			
R_1	0.0515	0.0353	0.0888	0.058	0.0497
wR_2 (all data)	0.1343	0.0873	0.2165	0.1231	0.1088
max electron density left (10^{-6} e/pm^3)	0.31	0.19	0.81	0.5	1.26

groups. For **4** three bands at 1988, 1864, and 1810 were recorded for the terminal CO groups; the related bands of **6** were located at 1991, 1854, and 1813 cm^{-1}, and the most intense middle bands of both compounds are relatively broad. The CO bands of the Mo complex **5** are more split showing bands at 2000, 1877 (with a shoulder at 1890), 1852, and 1806 cm^{-1} indicating a lower local symmetry. The low-frequency bands are consistent with the assumption that the chelating ligand is primarily a *σ*-donor, which concentrates electron density on the metal for back-bonding into the CO groups especially into those opposite to the sulfur atoms. Similar absorptions are found in the IR spectrum of the related complex $[(CO)_4MoS_2CN(Et_2)_2]^-$ (1993, 1868, 1828, 1783 cm^{-1}) which, according to the negative charge, are more shifted to lower frequencies.[18] Two strong bands at 1067 and 1099 cm^{-1} in **2** may be assigned to the vibration of the CS_2 moiety; similar strong peaks are found in the spectrum of the corresponding transition metal complexes (**4**, 1062 and 1100 cm^{-1}; **5**, 1067 and 1099 cm^{-1}; **6**, 1059 and 1100 cm^{-1}), but the majority of peaks in this region are originated from skeleton vibrations of the aromatic groups and prohibit an exact assignment.

Crystal Structures

General Remarks. To get more insight into the properties of the compounds and the structural change when the free ligand **2** is converted into the chelating ligand in **4**−**6** the molecular structures of all compounds have been determined by single-crystal X-ray diffraction measurements. Small crystals of **2** could be obtained by slow diffusion of a solution of CS_2 in THF into a THF solution of **1**. Colorless crystals of **3** could be obtained by admitting a THF solution of **1** to an atmosphere of dry CO_2. Orange crystals of **4**−**6** were grown from THF solutions by layering with pentane; the compounds **4** and **5** crystallize with two molecules of the solvent and are isotypical. The unit cell of **6** contains two independent formula units with one uncoordinated THF molecule. ORTEP views of the molecules are depicted in Figures 1 to 3. Details of the structure determinations are collected in Table 1; bond lengths and angles are summarized in the Tables 2−6.

Crystal Structure of the Adducts 2 and 3. In the crystal the two carbon atoms of **2** are located on a 2-fold axes. The structure is shown in Figure 1. The new C−C bond length amounts 147 pm and is the shortest among the carbon donating adducts **II**−**IV** and is shorter than a pure single bond; both carbon atoms are in an sp^2 hybridization state as proved by the sum of the angles amounting 360°. The planes between the *π*-systems CS_2 and CP_2 form an dihedral angle of 20°. Experimental and calculated (in italics) distances and

(18) Zhuang, B.; Huang, L.; He, L.; Yang, Y.; Lu, J. *Inorg. Chim. Acta* **1988**, *145*, 225.

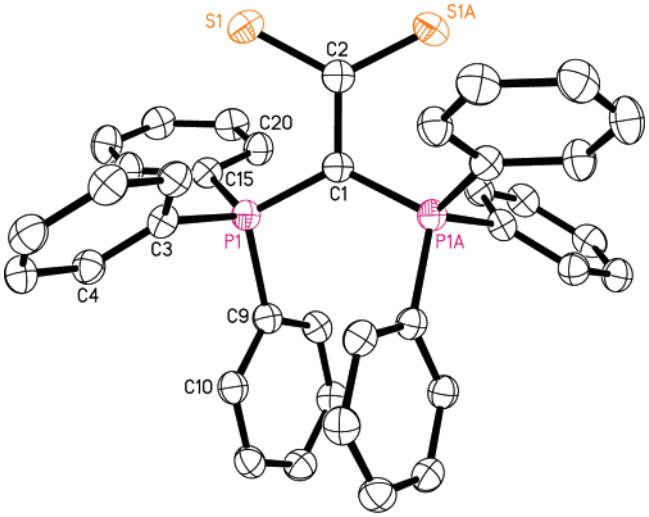

Figure 1. Crystal structure of $S_2CC(PPh_3)_2$ (**2**) showing the atom numbering scheme. The ellipsoids are drawn at a 40% probability level; the H atoms are omitted for clarity.

Table 2. Selected Experimental Distances and Angles of $S_2CC(PPh_3)_2$ (**2**)[a]

	Distances (pm)		
S(1)−C(2)	169.1(2)	P(1)−C(1)	175.1(2)
	170.2		*176.1*
P(1)−C(3)	181.5(3)	P(1)−C(9)	182.7(5)
	183.8		*185.1*
P(1)−C(15)	182.1(3)	C(1)−C(2)	146.9(6)
	183.6		*146.6*
	Angles (deg)		
C(1)−P(1)−C(3)	115.4(1)	C(1)−P(1)−C(9)	109.3(2)
	118.2		*111.0*
C(1)−P(1)−C(15)	111.8(1)	C(3)−P(1)−C(9)	106.3(1)
	110.8		*103.8*
C(3)−P(1)−C(15)	110.2(1)	C(9)−P(1)−C(15)	102.9(1)
	109.4		*102.2*
P(1)−C(1)−C(2)	116.4(1)	P(1)−C(1)−P(1A)	127.3(3)
	115.8		*128.4*
S(1)−C(2)−S(1A)	124.8(3)	S(1)−C(2)−C(1)	117.6(1)
	125.6		*117.2*
	Dihedral Angles (deg)		
S(1)−C(2)−C(1)−P(1)	20.0		
	25.8		

[a] Calculated values at B3LYP/III in italics.

angles are collected in Table 2. Comparing the structure of **2** with that of an electron-rich Arduengo carbene CS_2 adduct where the isolation of the π-systems is nearly perfect by a corresponding dihedral angle of 90° and of about 3−4 pm longer C−C bonds,[5,6] for **2** an additional but weak π-interaction between the two C atoms can be assumed. This is supported by the C−S distances which are ∼3 pm longer with respect to the distances in the related carbene adducts. Similarly, the C−P distances belong to the longest ones in this series of adducts. More strikingly in going from **1** to **2** the C−P distances have increased from 161 to 175 pm indicating decreasing back-donation of the occupied π-orbital at the carbon atom into σ^* antibonding orbitals at the P atoms. The S−C−S angle amounts to 125° and is more acute than that in the carbene adduct (129°). With respect to **1** the P−C−P angle has decreased from 134° to 127°. Although the geometrical parameter could be interpreted in favor of a bonding description of the zwitterionic moiety through that

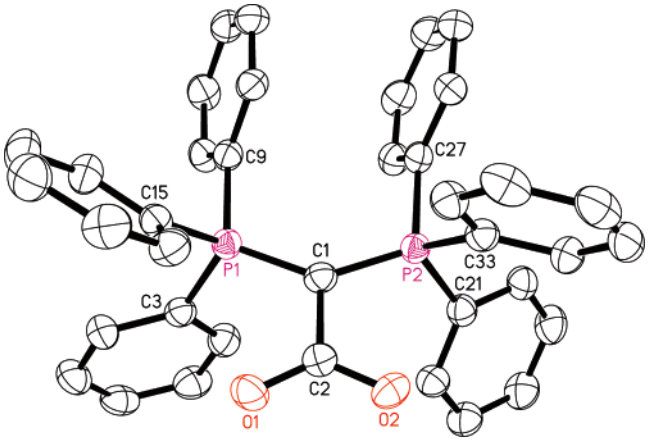

Figure 2. Crystal structure of $O_2CC(PPh_3)_2$ (**3**) showing the atom numbering scheme. The ellipsoids are drawn at a 40% probability level; the H atoms are omitted for clarity.

Scheme 3

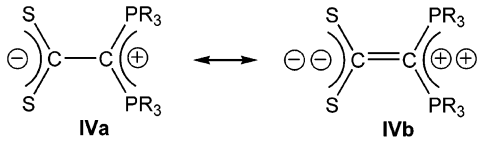

resonance structure **IVb** as depicted in Scheme 3 it will be shown in the theoretical part that the π-bonding contribution is rather small.

The molecular structure of **3** shown in Figure 2 is closely related to that of the CS_2−carbodiphosphorane adduct **2**, but the C−C bond length with 149 pm is slightly longer and the planes between the π-systems CO_2 and CP_2 form an dihedral angle of 10°, which is slightly more than the calculated one (3.1°). A similar bond length is recorded in the related carbene−CO_2 adduct, although the dihedral angle is 69°.[19] The C−P bond lengths amount to 172 pm, which are 3 pm shorter than those in **2**. Both carbon atoms are in a sp^2 hybridization state as shown by the sum of the angles. The C−O distances are 126 pm, which are 3 pm longer than in the corresponding carbene adduct.[19] Experimental and calculated (in italics) distances and angles are collected in Table 3.

The CE_2 adducts are compounds in which carbon−carbon bond formation has occurred during carbodiphosphorane addition to a Lewis acid. In comparing the structural data of **2** and **3** it becomes apparent, that the π-bonding between the two carbon atoms in **3** is less than in the CS_2 adduct **2**. It follows that the carbodiphosphorane **1** in the CO_2 adduct acts mainly as a σ-donor with less contribution of a π-interaction. The deviations of the dihedral angles from the favored and calculated (see below) planarity are probably steric in origin due to interactions with phenyl groups, which are more pronounced in the adduct containing the bulkier sulfur atoms. The bonding situation in **2** is studied in more detail using quantum theoretical methods as outlined in Theoretical Studies.

Crystal Structures of the Complexes 4−6. The crystal structure of the chromium complex **4** is depicted in Figure

(19) Kuhn, N.; Steinmann, M.; Weyers, G. *Z. Naturforsch.* **1999**, *54B*, 427.

Table 3. Selected Experimental Distances and Angles of $O_2CC(PPh_3)_2$ (**3**)[a]

	Distances (pm)		
P(1)−C(1)	172.1(2) *173.0*	P(1)−C(3)	180.9(2) *184.5*
P(1)−C(9)	180.4(2) *183.9*	P(1)−C(15)	182.7(2) *183.1*
P(2)−C(1)	171.4(3) *173.0*	P(2)−C(21)	182.6(2) *183.1*
P(2)−C(27)	181.0(2) *183.9*	P(2)−C(33)	181.2(2) *184.5*
O(1)−C(2)	125.8(3) *125.4*	O(2)−C(2)	126.0(3) *125.4*
C(1)−C(2)	149.4(3) *151.1*		
	Angles (deg)		
C(1)−P(1)−C(3)	110.6(1) *116.3*	C(1)−P(1)−C(9)	114.2(1) *113.9*
C(1)−P(1)−C(15)	114.6(1) *111.4*	C(3)−P(1)−C(9)	105.1(1) *101.9*
C(3)−P(1)−C(15)	108.6(1) *107.7*	C(9)−P(1)−C(15)	103.0(1) *104.5*
C(1)−P(2)−C(21)	115.2(1) *111.4*	C(1)−P(2)−C(27)	114.6(1) *113.9*
C(1)−P(2)−C(33)	110.4(1) *116.3*	C(21)−P(2)−C(27)	100.6(1) *104.5*
C(21)−P(2)−C(33)	109.6(1) *107.7*	C(27)−P(2)−C(33)	105.7(1) *101.9*
P(1)−C(1)−C(2)	112.7(2) *110.7*	P(1)−C(1)−P(2)	135.2(1) *138.6*
P(2)−C(1)−C(2)	111.6(2) *110.7*	O(1)−C(2)−O(2)	127.7(2) *129.5*
O(1)−C(2)−C(1)	117.4(2) *115.3*	O(2)−C(2)−C(1)	114.9(2) *115.3*
	Dihedral Angles (deg)		
O(1)−C(2)−C(1)−P(1)	10.0 *3.1*		

[a] Calculated values at B3LYP/III in italics.

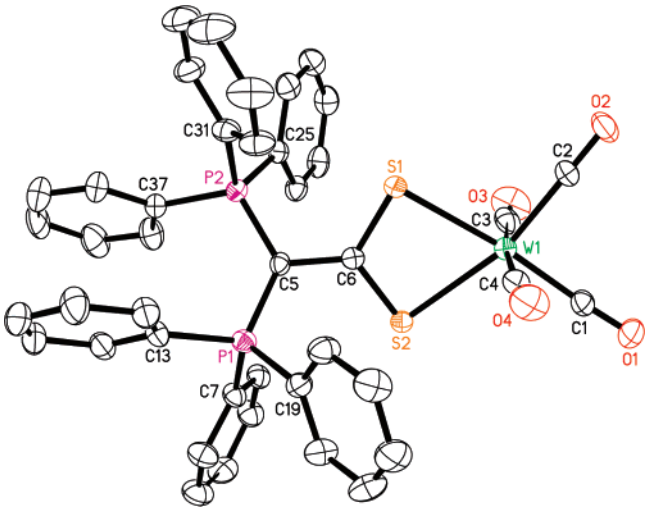

Figure 3. Crystal structure of $[(CO)_4WS_2CC(PPh_3)_2]$ (**6**) showing the atom numbering scheme. The ellipsoids are drawn at a 40% probability level; the H atoms and the disordered THF molecules are omitted for clarity. See Table 6.

3. The crystal structure of the molybdenum complex **5** is isotypic to **4** and therefore it is not shown. Selected bond lengths and angles are shown in Tables 4 and 5. The compounds crystallize with two disordered THF molecules; no disorder is found in the metal-containing molecules and the disordered THF molecules were refined with split functions of 0.4 and 0.6. The crystal structure of the tungsten complex **6** is very similar to **4** and **5** and therefore it is not shown. The geometrical data are given in Table 6; two independent formula units were found with one uncoordinated THF molecule.

Table 4. Selected Experimental Distances and Angles of the Chromium Complex **4**

	Distances (pm)		
Cr(1)−S(1)	243.2(2)	Cr(1)−S(2)	247.1(3)
Cr(1)−C(1)	179(1)	Cr(1)−C(2)	180(1)
Cr(1)−C(3)	188.5(9)	Cr(1)−C(4)	185.0(9)
S(1)−C(6)	168.9(8)	S(2)−C(6)	170.5(8)
P(1)−C(5)	174.7(8)	P(1)−C(7)	181.0(8)
P(2)−C(5)	175.5(8)	P(2)−C(25)	182.2(8)
P(2)−C(31)	181.5(8)	P(2)−C(37)	182.3(8)
O(1)−C(1)	118(1)	O(2)−C(2)	119(1)
O(3)−C(3)	117(1)	O(4)−C(4)	118(1)
C(5)−C(6)	145(1)		
	Angles (deg)		
S(1)−Cr(1)−S(2)	70.61(8)	S(1)−Cr(1)−C(1)	95.6(3)
S(1)−Cr(1)−C(2)	171.4(3)	S(1)−Cr(1)−C(3)	90.1(3)
S(1)−Cr(1)−C(4)	92.7(3)	S(2)−Cr(1)−C(1)	165.8(3)
S(2)−Cr(1)−C(2)	101.1(3)	S(2)−Cr(1)−C(3)	89.4(3)
S(2)−Cr(1)−C(4)	91.1(3)	C(1)−Cr(1)−C(2)	92.8(4)
C(1)−Cr(1)−C(3)	87.1(4)	C(1)−Cr(1)−C(4)	93.0(4)
C(2)−Cr(1)−C(3)	92.3(4)	C(2)−Cr(1)−C(4)	84.9(4)
C(3)−Cr(1)−C(4)	177.2(4)	Cr(1)−S(1)−C(6)	88.9(3)
Cr(1)−S(2)−C(6)	87.3(3)	P(1)−C(5)−P(2)	124.1(4)
P(1)−C(5)−C(6)	116.6(5)	P(2)−C(5)−C(6)	119.3(6)
S(1)−C(6)−S(2)	113.2(4)	S(1)−C(6)−C(5)	123.0(6)
S(2)−C(6)−C(5)	123.8(6)		

On complex formation, **2** acts as a chelating ligand and the coordination to the metal atoms occurs via the two sulfur atoms occupying two sites in the octahedral arrangement. The geometry around the metal atoms is a distorted octahedron with small S−M−S angles of 67−70°. In going from the free ligand **2** to the complexes **4**−**6** an electron release from the ligand to the metal fragment is induced which, however, causes no dramatical change of the geometrical parameters at the ligand. Thus, the C−C bond lengths decrease by ∼2 pm, indicating more π-interaction, while the C−S and the C−P distances show only a slight tendency to increase. Upon complex formation the contribution of resonance form **IVb** becomes more important. The bite angles of the chelating CS_2 group decrease by about 10−12°, while the P−C−P angles remain nearly unchanged. The four membered M−S−C−S rings are planar and the dihedral angle of the free ligand has increased by 12° in all complexes. This further deviation of the two π-systems from planarity may be due to packing effects. The trans effect of

(20) Sheldrick, G. M.; SHELXTL, Release 5.05/VMS for Siemens R3 Crystallographic Research System, Siemens Analytical x-ray Instruments Inc.; Madison, WI, 1996.
(21) Sheldrick, G. M.; SHELXS-97, Göttingen 1997.
(22) Sheldrick, G. M.; SHELXL-97, Göttingen 1997.
(23) Altomare, A.; Cascarano, G.; Giacovazzo, C.; Guagliardi, A.; Burla, M. C.; Polidori, G.; Camalli, M., SIR-92, Rome, 1992.
(24) (a) Becke, A. D. *J. Chem. Phys.* **1993**, *98*, 5648. (b) Lee, C.; Yang, W.; Parr, R. G. *Phys. Rev. B* **1988**, *37*, 785. (c) Stevens, P. J.; Devlin, F. J.; Chablowski, C. F.; Frisch, M. J. *J. Phys. Chem.* **1994**, *98*, 11623.
(25) (a) Becke, A. D. *Phys. Rev. A* **1988**, *38*, 3098. (b) Perdew, J. P. *Phys. Rev. B* **1986**, *33*, 8822.
(26) Hay, P. J.; Wadt, W. R. *J. Chem. Phys.* **1985**, *82*, 299.
(27) (a) Ditchfield, R.; Hehre, W. J.; Pople, J. A. *J. Chem. Phys.* **1971**, *54*, 724. (b) Hehre, W. J.; Ditchfield, R.; Pople, J. A. *J. Chem. Phys.* **1972**, *56*, 2257.
(28) Frenking, G.; Antes, I.; Böhme, M.; Dapprich, S.; Ehlers, A. W.; Jonas, V.; Neuhaus, A.; Otto, M.; Stegmann, R.; Veldkamp, A.; Vyboishchikov, S. F. In *Reviews in Computational Chemistry*; Lipkowitz, K. B., Boyd, D. B., Eds.; VCH: New York, 1996; Vol. 8, pp 63−144.

Table 5. Selected Experimental Distances and Angles of the Molybdenum Complex **5**[a]

	Distances (pm)		
Mo(1)−S(1)	255.8(1) *274.7*	Mo(1)−S(2)	260.7(1) *274.7*
Mo(1)−C(1)	193.9(6) *197.2*	Mo(1)−C(2)	193.8(7) *197.2*
Mo(1)−C(3)	201.8(7) *206.2*	Mo(1)−C(4)	201.0(7) *206.2*
S(1)−C(6)	170.3(5) *169.6*	S(2)−C(6)	170.7(5) *169.6*
P(1)−C(5)	175.8(5) *172.1*	P(1)−C(7)	181.1(5)
P(1)−C(13)	181.2(5)	P(1)−C(19)	180.0(5)
P(2)−C(5)	175.2(5) *172.1*	P(2)−C(25)	180.0(5)
P(2)−C(31)	181.9(5)	P(2)−C(37)	181.0(5)
O(1)−C(1)	117.4(7) *115.5*	O(2)−C(2)	118.3(7) *115.5*
O(3)−C(3)	115.5(7) *114.7*	O(4)−C(4)	116.0(7) *114.7*
C(5)−C(6)	144.9(7) *144.1*		
	Angles (deg)		
S(1)−Mo(1)−S(2)	67.63(4) *65.3*	S(1)−Mo(1)−C(1)	98.2(2) *102.0*
S(1)−Mo(1)−C(2)	170.9(2) *167.3*	S(1)−Mo(1)−C(3)	90.3(2) *92.2*
S(1)−Mo(1)−C(4)	92.3(2) *92.2*	S(2)−Mo(1)−C(1)	165.5(2) *167.3*
S(2)−Mo(1)−C(2)	103.5(2) *102.0*	S(2)−Mo(1)−C(3)	88.8(2) *92.2*
S(2)−Mo(1)−C(4)	92.3(2) *92.2*	C(1)−Mo(1)−C(2)	90.8(3) *90.7*
C(1)−Mo(1)−C(3)	88.5(2) *88.2*	C(1)−Mo(1)−C(4)	91.1(3) *88.2*
C(2)−Mo(1)−C(3)	91.5(3) *88.2*	C(2)−Mo(1)−C(4)	85.8(3) *88.2*
C(3)−Mo(1)−C(4)	177.3(2) *174.8*	Mo(1)−S(1)−C(6)	89.6(2) *86.5*
Mo(1)−S(2)−C(6)	87.9(2) *86.5*	P(1)−C(1)−P(2)	123.8(3) *127.4*
Mo(1)−C(2)−O(2)	176.3(6) *179.6*	Mo(1)−C(5)−O(3)	176.5(6) *179.6*
Mo(1)−C(4)−O(4)	174.6(6) *176.3*	Mo(1)−C(3)−O(3)	178.2(5) *176.3*
P(1)−C(5)−C(6)	116.5(3) *116.3*	P(2)−C(5)−C(6)	119.6(4) *116.3*
S(1)−C(6)−S(2)	115.0(3) *121.8*	S(1)−C(6)−C(5)	122.1(4) *119.1*
S(2)−C(6)−C(1)	123.0(3) *119.1*		
	Dihedral Angles (deg)		
S(1)−C(6)−C(1)−P(1)	32.0 *0.0*		

[a] Calculated values of the model compound **5M** with R = H at B3LYP/III in italics.

the chelating ligand shortens the opposite M−$C_{carbonyl}$ bond and elongates the corresponding C−O bond, which is consistent with a higher σ-donor/π-acceptor ratio of the sulfur atoms of **2** relative to CO. In the ylide adduct complex $[(CO)_3BrMnS_2CC(Me_2)PPh_3]$, containing an sp^3 donor carbon atom, similar parameters are found in the CS_2 part of the molecule but a long C−C distance typical for a normal single bond was recorded.[8a] The average M−S distances increase down the periodic table as expected from Cr (245 pm) to Mo (258 pm) and, according to relativistic effects, remains unchanged in W (258 pm), thus following the trend in covalent radii.

Table 6. Selected Experimental Distances and Angles of the Tungsten Complex **6**

	Distances (pm)		
W(1)−S(1)	256.1(2)	W(1)−S(2)	259.3(2)
W(1)−C(1)	193.8(8)	W(1)−C(2)	195.7(8)
W(1)−C(3)	200.7(9)	W(1)−C(4)	204.8(9)
S(1)−C(6)	169.9(8)	S(2)−C(6)	170.3(7)
P(1)−C(5)	174.6(7)	P(1)−C(7)	181.7(8)
P(1)−C(13)	182.1(8)	P(1)−C(19)	181.9(8)
P(2)−C(5)	175.8(7)	P(2)−C(25)	181.5(7)
O(1)−C(1)	117.6(9)	O(2)−C(2)	117.0(9)
O(3)−C(3)	118(1)	O(4)−C(4)	115(1)
C(5)−C(6)	147(1)		
	Angles (deg)		
S(1)−W(1)−S(2)	67.26(8)	S(1)−W(1)−C(1)	173.9(3)
S(1)−W(1)−C(2)	96.5(3)	S(1)−W(1)−C(3)	94.9(2)
S(1)−W(1)−C(4)	91.3(2)	S(2)−W(1)−C(1)	107.4(3)
S(2)−W(1)−C(2)	163.7(3)	S(2)−W(1)−C(3)	94.5(2)
S(2)−W(1)−C(4)	90.4(2)	C(1)−W(1)−C(2)	88.8(4)
C(1)−W(1)−C(3)	88.4(3)	C(1)−W(1)−C(4)	85.6(3)
C(2)−W(1)−C(3)	87.7(3)	C(2)−W(1)−C(4)	89.0(3)
C(3)−W(1)−C(4)	173.2(3)	W(1)−S(1)−C(6)	89.8(2)
W(1)−S(2)−C(6)	88.7(3)	P(1)−C(5)−P(2)	125.8(4)
P(1)−C(5)−C(6)	118.8(5)	P(2)−C(5)−C(6)	115.3(5)
S(1)−C(6)−S(2)	114.1(4)	S(1)−C(6)−C(5)	123.1(5)
S(2)−C(6)−C(5)	122.7(6)		

Theoretical Studies

We calculated the geometries and bond dissociation energies (BDEs) of the carbodiphosphorane adducts with CS_2 (**2**) and CO_2 (**3**) ligands using DFT (B3LYP, BP86) and ab initio (MP2) methods with basis sets having valence TZ2P quality. We calculated also a model compound of the molybdenum complex **5** where the phenyl groups are substituted by hydrogen, i.e., $[(CO)_4MoS_2CC(PH_3)_2]$ (**5M**). The bonding situation of **2**, **3**, and **5M** has been investigated with charge and energy decomposition methods. The technical details are given in the method section.

Geometries and Energies. Tables 2, 3, and 5 give the most important theoretical bond lengths and angles of the

(29) Møller, C.; Plesset, M. S. *Phys. Rev.* **1934**, *46*, 618.
(30) Reed, A. E.; Curtiss, L. A.; Weinhold, F. *Chem. Rev.* **1988**, *88*, 899.
(31) (a) Gaussian98 (Revision A.1): Frisch, M. J.; Trucks, G. W.; Schlegel, H. B.; Scuseria, G. E.; Robb, M. A.; Cheeseman, J. R.; Zakrzewski, V. G.; Montgomery, J. A.; Stratmann, R. E.; Burant, J. C.; Dapprich, S.; Milliam, J. M.; Daniels, A. D.; Kudin, K. N.; Strain, M. C.; Farkas, O.; Tomasi, J.; Barone, V.; Cossi, M.; Cammi, R.; Mennucci, B.; Pomelli, C.; Adamo, C.; Clifford, S.; Ochterski, J.; Petersson, G. A.; Ayala, P. Y.; Cui, Q.; Morokuma, K.; Malick, D. K.; Rabuck, A. D.; Raghavachari, K.; Foresman, J. B.; Cioslowski, J.; Ortiz, J. V.; Stefanov, B. B.; Liu, G.; Liashenko, A.; Piskorz, P.; Komaromi, I.; Gomberts, R.; Martin, R. L.; Fox, D. J.; Keith, T. A.; Al-Laham, M. A.; Peng, C. Y.; Nanayakkara, A.; Gonzalez, C.; Challacombe, M.; Gill, P. M. W.; Johnson, B. G.; Chen, W.; Wong, M. W.; Andres, J. L.; Head-Gordon, M.; Replogle, E. S.; Pople, J. A. Gaussian Inc., Pittsburgh, PA 1998. (b) Gaussian03 (Revision B.05): Frisch, M. J.; Trucks, G. W.; Schlegel, H. B.; Scuseria, G. E.; Robb, M. A.; Cheeseman, J. R.; Montgomery, J. A., Jr.; Vreven, T.; Kudin, K. N.; Burant, J. C.; Milliam, J. M.; Iyengar, S. S.; Tomasi, J.; Barone, V.; Mennucci, B.; Cossi, M.; Scalmani, G.; Rega, N.; Petersson, G. A.; Nakatsuji, H.; Hada, M.; Ehara, M.; Toyota, K.; Fukuda, R.; Hasegawa, J.; Ishida, M.; Nakajima, T.; Honda, Y.; Kitao, O.; Nakai, H.; Klene, M.; Li, X.; Knox, J. E.; Hratchian, H. P.; Cross, J. B.; Adamo, C.; Jaramillo, J.; Gomperts, R.; Stratmann, R. E.; Yazyev, O.; Austin, A. J.; Cammi, R.; Pomelli, C.; Ochterski, J. W.; Ayala, P. Y.; Morokuma, K.; Voth, G. A.; Salvador, P.; Dannenberg, J. J.; Zakrzewski, V. G.; Dapprich, S.; Daniels, A. D.; Strain, M. C.; Farkas, O.; Malick, D. K.; Rabuck, A. D.; Raghavachari, K.; Foresman, J. B.; Ortiz, J. V.; Cui, Q.; Baboul, A. G.; Clifford, S.; Cioslowski, J.; Stefanov, B. B.; Liu, G.; Liashenko, A.; Piskorz, P.; Komaromi, I.; Martin, R. L.; Fox, D. J.; Keith, T.; Al-Laham, M. A.; Peng, C. Y.; Nanayakkara, A.; Challacombe, M.; Gill, P. M. W.; Johnson, B.; Chen, W.; Wong, C.; Gonzalez, M. W.; Pople, J. A. Gaussian, Inc., Pittsburgh, PA, 2003.

compounds **2**, **3**, and **5M**, which were calculated at the B3LYP/III level. The agreement between the experimental and calculated values for **2** and **3** is very good. The calculated value of the Mo−S bonds of **5M** (274.7 pm) is longer than the experimental data for **5** (255.8(1) and 260.7(1) pm), but the shorter bonds that are found by X- ray-structure analysis may be partly caused by packing effects. Theoretical and experimental studies have shown that donor−acceptor bonds in the solid state are always shorter than in the gas phase due to intermolecular interactions.[40] This may hold in particular for donor−acceptor bonds of the soft sulfur atom. Theory and experiment indicate that the C−C donor−acceptor bond in the metal complex **5** (**5M**) is shorter than in the adducts **2** and **3** and that the CO_2 adduct **3** has a longer donor−acceptor bond than the CS_2 adduct **2**. The calculated acute bending angles of the CS_2 and CO_2 moieties in **2** (125.6°) and **3** (129.5°) are in very good agreement with the experimental values of 124.8(3)° and 127.7(2)°, respectively.

The calculated equilibrium geometry of **2** shows that the CS_2 acceptor fragment is rotated 25.8° from the plane of the carbodiphosphorane donor. This complies with the experimentally obtained dihedral angle of 20°. Theory and experiment agree that the CO_2 fragment in **3** is less rotated from the plane of the donor moiety. The calculated value for the dihedral angle is 3.1° while the measured value is 10°. The experimentally observed rotation of the CS_2 fragment from the plane of the diphosphorane moiety in the complex **5** increases by 12° compared with **2** while the calculated dihedral angle in **5M** is zero. The difference can be explained with steric effects (use of the smaller PH_3 groups in the model compound) and with packing forces in the experimental structure. Geometry optimizations of **2** and **3** where the fragments CX_2 and $C(Ph_3)_2$ are enforced to be coplanar suggest that the energy differences between the planar and equilibrium structures are very small. The theoretical values for the energy differences are 0.23 kcal/mol for **2** and 0.03 kcal/mol for **3**. The rotational barriers of **2** and **3** where the CS_2 and CO_2 groups are perpendicular to the carbodiphosphorane plane are higher. The calculated values at B3LYP/III, which indicate the strength of the π-interactions are 7.0 kcal/mol for **2** and 9.4 kcal/mol for **3**.

Table 7. Calculated Bond Dissociation Energies D_e and ZPE Corrected Values D_o (kcal/mol)[a]

		B3LYP/III// B3LYP/III		BP86/TZ2P// BP86/TZ2P		MP2/III// B3LYP/III	
molecule	bond	D_e	D_o	D_e	D_o	D_e	D_o
2	C1−C2	5.1	3.3	6.0	4.1	30.7	28.8
3	C1−C2	2.2	−0.1	1.5	−0.8	13.4	11.1
5M	C5−C6	36.3	33.2	36.0	32.9	43.2	40.1
	Mo−S	32.4	31.7	36.7	36.0	58.1	57.4

[a] The ZPE corrections are taken from B3LYP/II calculations.

We calculated the BDEs of the C−C bonds of **2**, **3**, and **5M** and the BDE of the Mo−S bonds of **5M** at B3LYP/III//B3LYP/III, BP86/TZ2P//BP86/TZ2P and MP2/III//B3LYP/III. The results are shown in Table 7. It becomes obvious that DFT underestimates the strength of the C−C bonds particularly for compounds **2** and **3**.[43] The hybrid functional B3LYP and the pure DFT functional BP86 predict that both molecules have very small bond dissociation energies. The theoretical value for **2** at B3LYP/III is only $D_o = 3.3$ kcal/mol. BP86/TZ2P gives a slightly higher value $D_o = 4.1$ kcal/mol. For **3**, B3LYP/III ($D_o = -0.1$ kcal/mol) and BP86/III ($D_o = -0.8$ kcal/mol) give negative values for the BDE at 0 K. It follows that the DFT methods are not reliable for the calculation of the thermodynamic stability of **2** and **3**. The theoretically predicted BDEs of both complexes at MP2/III are much higher. The calculated values for **2** ($D_o = 28.8$ kcal/mol) and **3** ($D_o = 11.1$ kcal/mol) are in agreement with the experimental result that both compounds can be isolated and that the CO_2 adduct **3** is less stable than **2**.

The DFT methods give also smaller values for the BDE of the C−C bond of **5M** than MP2. The calculated data at B3LYP/III ($D_o = 33.2$ kcal/mol) and BP86/TZ2P ($D_o = 32.9$ kcal/mol) indicate weaker bonds than the MP2 value ($D_o = 40.1$ kcal/mol). All theoretical methods agree, however, that the C−C bond of **2** becomes much stronger when the molecule is bonded to $Mo(CO)_4$. The theoretically predicted BDE of the metal−sulfur bonds $(CO)_4Mo-$**2** of **5M** at MP2/III is $D_o = 57.4$ kcal/mol. This is much higher than the DFT values at B3LYP/III ($D_o = 31.7$ kcal/mol) and BP86/TZ2P ($D_o = 36.0$ kcal/mol). We think that the MP2 value is more reliable than the DFT data.

Another way for estimating the BDE of the $(CO)_4Mo-$**2** metal−sulfur bonds is by calculating the reaction energy of the isostructural[41] reaction 1:

$$Mo(CO)_6 + \mathbf{2M} \rightarrow \mathbf{5M} + 2CO \qquad (1)$$

The calculated reaction energy for reaction 1 gives the relative BDE of ligand **2M** with respect to two CO ligands.

(32) (a) Baerends, E. J.; Ellis, D. E.; Ros, P. *Chem. Phys.* **1973**, *2*, 41. (b) Versluis, L.; Ziegler, T. *J. Chem. Phys.* **1988**, *322*, 88. (c) te Velde, G.; Baerends, E. J. *J. Comput. Phys.* **1992**, *99*, 84. (d) Fonseca Guerra, C.; Snijders, J. G.; te Velde, G.; Barends, E. J. *Theor. Chim. Acta* **1998**, *99*, 391.

(33) (a) Bickelhaupt, F. M.; Baerends, E. J. In *Review of Computational Chemistry;* Lipkowitz, K. B., Boyd, D. B., Eds.; Wiley-VCH: New York, 2000;Vol. 15, p 1. (b) te Velde, G.; Bickelhaupt, F. M.; Baerends, E. J.; van Gisbergen, S. J. A.; Fonseca Guerra, C.; Snijders, J. G.; Ziegler, T. *J. Comput. Chem.* **2001**, *22*, 931.

(34) Morokuma, K. *J. Chem. Phys.* **1971**, *55*, 1236.

(35) Ziegler, T.; Rauk, A. *Theor. Chim. Acta* **1977**, *46*, 1.

(36) Snijders, J. G.; Baerends, E. J.; Vernooijs, P. *At. Nucl. Data Tables* **1982**, *26*, 483.

(37) (a) Chang, C.; Pelissier, M.; Durand, Ph. *Phys. Scr.* **1986**, *34*, 394. (b) Heully, J.-L.; Lindgren, I.; Lindroth, E.; Lundquist, S.; Martensson-Pendrill, A.-M. *J. Phys. B* **1986**, *19*, 2799. (c) van Lenthe, E.; Baerends, E. J.; Snijders, J. G. *J. Chem. Phys.* **1993**, *99*, 4597. (d) van Lenthe, E.; Baerends, E. J.; Snijders, J. G. *J. Chem. Phys.* **1996**, *105*, 6505. (c) van Lenthe, E.; van Leeuwen, R.; Baerends, E. J.; Snijders, J. G. *Int. J. Quantum Chem.* **1996**, *57*, 281.

(38) (a) Baerends, E. J.; Ellis, D. E.; Ros, P. *Chem. Phys.* **1973**, *2*, 41. (b) Krijn, J.; Baerends, E. J. *Fit Functions in the HFS-Method*, Internal Report (in dutch), Vrije Universiteit Amsterdam, The Netherlands, 1984.

(39) Frenking, G.; Wichmann, K.; Fröhlich, N.; Loschen, C.; Lein, M.; Frunzke, J.; Rayón, V. M. *Coord. Chem. Rev.* **2003**, *238*−*239*, 55.

(40) Jonas, J.; Frenking, G.; Reetz, M. T. *J. Am. Chem. Soc.* **1994**, *116*, 8741.

(41) Dapprich, S.; Pidun, U.; Ehlers, A. W.; Frenking, G. *Chem. Phys. Lett.* **1995**, *242*, 521.

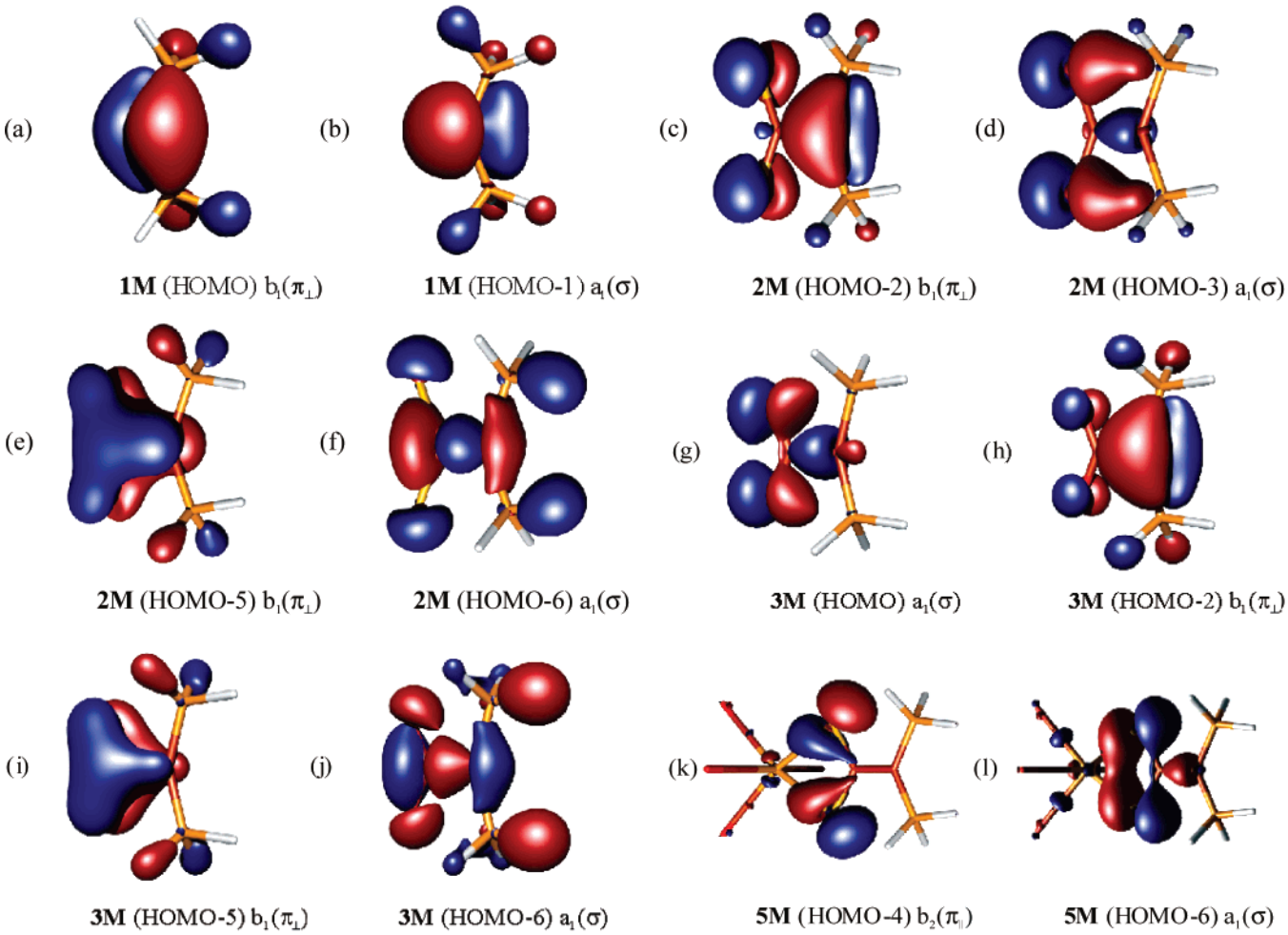

Figure 4. Plot of the σ- and π-orbitals which are relevant for the donor−acceptor bonding in the CS_2 and CO_2 complexes of **1**. (a) HOMO of **1**. (b) HOMO-1 of **1**. (c) HOMO-2 of **2M**. (d) HOMO-3 of **2M**. (e) HOMO-5 of **2M**. (f) HOMO-6 of **2M**. (g) HOMO of **3M**. (h) HOMO-2 of **3M**. (i) HOMO-5 of **3M**. (j) HOMO-6 of **3M**. (k) HOMO-6 of **5M**. (l) HOMO-12 of **5M**.

The calculated values at B3LYP/III are $\Delta D_e = 38.1$ kcal/mol and $\Delta D_o = 34.9$ kcal/mol. Slightly higher values are calculated at BP86/TZ2P ($\Delta D_e = 42.2$ kcal/mol, $\Delta D_o = 39.0$ kcal/mol). The MP2/III values are $\Delta D_e = 33.7$ kcal/mol and $\Delta D_o = 30.5$ kcal/mol. The latter value predict that the ligand **2M** in complex **5M** is 30.5 kcal/mol weaker bonded than two CO groups in $Mo(CO)_6$. This may also be used for estimating the relative bond energy of **2** assuming that the effect of substituting PPh_3 with PH_3 in **2M** and **5M** cancels.

Bonding Analysis. A reasonable starting point for analyzing the donor−acceptor bonds in **2** and **3** is the electronic structure of the donor species carbodiphosphorane (**1**). To facilitate the qualitative orbital analysis of the donor−acceptor interactions in **2** and **3** we used the model compounds **1M**, **2M**, and **3M** optimized with C_{2v} symmetry constraint where the PPh_3 groups are substituted by PH_3. Calculations of the structures showed that the geometries are very similar to those of **1**−**3**. Orbitals a and b in Figure 4 show the two highest occupied MOs of **1M**.

The shape of the molecular orbitals indicates that the HOMO *and* the HOMO-1 of **1M** are both lone-pair orbitals of the carbon atom. The HOMO is mainly an out-of-plane ($\pi_\perp$) orbital and the HOMO-1 is a sp-hybridized σ-orbital. The NBO analysis gives also two lone-pair orbitals at carbon, a π-lone-pair orbital (occupation 1.630) and a σ-lone-pair orbital (occupation 1.553). The hybridization in the σ-lone-pair orbital is $sp^{2.1}$. The NBO method suggests that the carbon−phosphorus bonds come from donation of the phosphorus electron lone pairs of the PH_3 moieties into the empty carbon AOs. There are three P−H orbitals and one P−C orbital but there is no phosphorus lone-pair orbital. Carbodiphosphoranes should therefore be considered as double electron pair donors, i.e., they are σ-and π-donors. The calculated atomic partial charges support the bonding picture, which suggests a large charge concentration at the carbon atom. The calculated NBO value of **1M** at B3LYP/III is $q(C) = -1.44$ e while the partial charge at phosphorus is $q(P) = +0.91$ e.

Orbitals c−f in Figure 4 show also the occupied molecular orbitals of **2M**, which are relevant for the C−C bonding interactions. The HOMO and HOMO-1 are sulfur in-plane and out-of-plane lone-pair orbitals, and therefore, they are

(42) Arduengo, A. J., III; Harlow, R. L.; Kline, M. *J. Am. Chem. Soc.* **1991**, *113*, 361.
(43) The problem of DFT for giving reliable BDE values for donor−acceptor complexes has recently been described by: Gilbert, T. M. *J. Phys. Chem. A* **2004**, *108*, 2550.

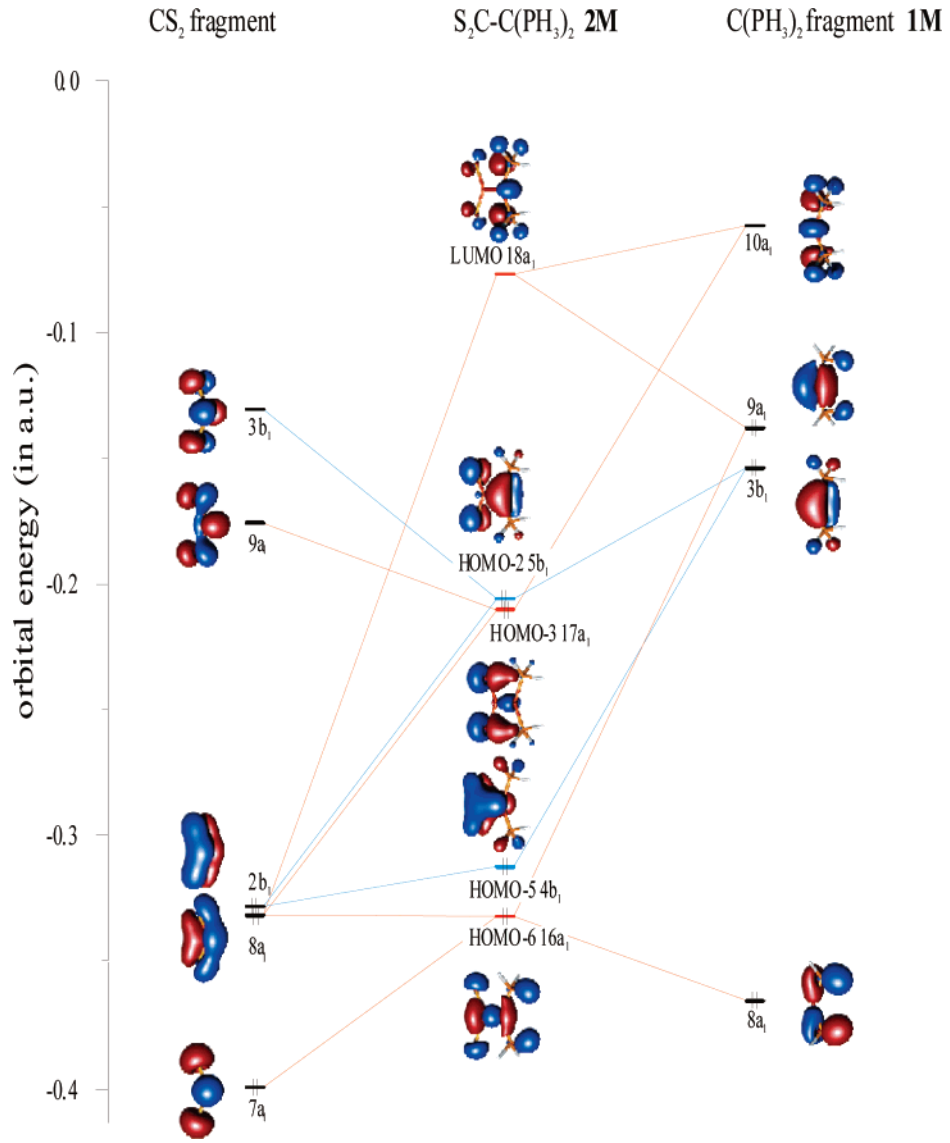

Figure 5. Orbital correlation diagram for the interactions between the $C(PH_3)_2$ donor and CS_2 acceptor in $S_2CC(PH_3)_2$ (**2M**). Only the most important σ (a_1) and $\pi_\perp$ (b_1) orbitals are shown.

not shown. The HOMO-2 (Figure 4c) and HOMO-5 (Figure 4e) are the highest occupied b_1 orbitals that are associated with the C−C out-of-plane ($\pi_\perp$) bonding. HOMO-3 (Figure 4d) and HOMO-6 (Figure 4f) are the highest occupied a_1 orbitals associated with the C−C σ-bonding. Figure 5 displays an orbital correlation diagram for the C−C σ- and $\pi_\perp$-orbitals of **2M**. It shows the results of the fragment orbital analysis of the program ADF,[32,33] which uses a linear combination of the fragment orbitals for building the MOs of a molecule.

From the shape of the $\pi_\perp$ orbitals HOMO-5 of **2M** and $2b_1$ of CS_2 it appears as if π-charge is donated from the CS_2 ligand to the carbodiphosphorane **1M**. The visual impression is misleading, however. The fragment orbital analysis shows that the occupied $\pi_\perp$-orbitals HOMO-3 and HOMO-5 of **2M** come mainly from the mixing of two occupied orbitals, i.e., $2b_1$ of CS_2 and $3b_1$ of **1M**, with one vacant $3b_1$ orbital of CS_2. This gives an overall $\pi_\perp$-charge donation in the direction **1M** → CS_2. The conclusion is supported by the calculated partial charges (Table 8). The electronic partial charge in the b_1 ($\pi_\perp$) orbitals of the CS_2 fragment of **2M** is $\Delta q(\pi_\perp) = -0.19$ e. But CS_2 is also a σ-acceptor in **2M**. The total partial charge of the CS_2 fragment is $\Delta q = -0.66$ e. This means that the **1M** → CS_2 σ-donation is 0.43 e because the contributions of a_2 (δ) and b_2 ($\pi_{||}$) charge donation are negligible (Table 8). The calculated NBO charges of **2M** agree with the notation that the carbodiphosphorane **1M** is

Table 8. Calculated Differences of the NBO Partial Charges of the Fragments CX_2 and $Mo(CO)_4$ at B3LYP/III

molecule	$\Delta q_{a1}(\sigma)$	$\Delta q_{a2}(\delta)$	$\Delta q_{b1}(\pi_\perp)$	$\Delta q_{b2}(\pi_{||})$	$\Sigma\,\Delta q$
2M[a]	−0.43	0.00	−0.19	−0.03	−0.66
3M[a]	−0.54	0.00	−0.07	−0.07	−0.68
5M[b]	−0.20	0.00	0.07	−0.24	−0.37

[a] $\Delta q_{\pi/\sigma/\delta}$ gives the occupancy differences of the orbitals of CX_2 with $\pi/\sigma/\delta$ symmetry between the free fragments and CX_2 ligands in the complexes (X = S, O). Negative numbers mean that the partial charges of the ligands in the complexes are larger than in the free molecule. [b] $\Delta q_{\pi/\sigma/\delta}$ gives the occupancy differences of the orbitals of $Mo(CO)_4$ with $\pi/\sigma/\delta$ symmetry between the free molecule and the metal fragment in the complex. Negative numbers mean that the partial charges of the metal fragment in the complex are larger than in the free molecule.

Table 9. Energy Partitioning Analysis of the Donor−Acceptor Bonds for the Planar (C_{2v}) Structures of Compounds **2**−**5M**[a]

	2	**2M**	**3**	**3M**	**2Ar**	**5M**	**5M**
bond	C−C	C−C	C−C	C−C	C−C	C−C	Mo−S
ΔE_{int}	−78.3	−93.3	−63.3	−70.9	−64.4	−96.8	−45.8
ΔE_{Pauli}	574.7	654.7	423.4	491.2	499.6	513.3	65.7
ΔE_{elstat}[b]	−268.0 (41.0)	−298.6 (39.9)	−213.1 (43.8)	−241.4 (42.9)	−245.0 (43.4)	−250.2 (41.0)	−60.8 (54.6)
ΔE_{orb}[b]	−385.0 (59.0)	−449.4 (60.1)	−273.6 (56.2)	−320.7 (57.1)	−319.1 (56.6)	−360.0 (59.0)	−50.7 (45.4)
ΔE_{σ} (a_1)[c]	−317.0 (82.3)	−379.9 (84.5)	−226.8 (82.9)	−267.2 (83.3)	−284.7 (89.2)	−304.5 (84.6)	−20.7 (40.8)
ΔE_{δ} (a_2)[c]	−3.6 (0.9)	−2.4 (0.5)	−4.0 (1.4)	−3.1 (1.0)	−1.6 (0.5)	−2.5 (0.7)	−2.1 (4.2)
$\Delta E\pi_{\perp}$ (b_1)[c]	−40.0 (10.4)	−38.8 (8.6)	−25.6 (9.3)	−25.9 (8.1)	−21.4 (6.7)	−35.5 (9.9)	−6.4 (12.6)
$\Delta E\pi_{\parallel}$ (b_2)[c]	−24.3 (6.3)	−28.4 (6.3)	−17.3 (6.3)	−24.6 (7.7)	−11.5 (3.6)	−17.5 (4.9)	−21.5 (42.3)
ΔE_{prep}	78.7	65.1	68.1	61.5	57.1	60.8	9.2
ΔE (= $-D_e$)	0.3	−28.3	4.7	−9.4	−7.3	−36.0	−36.6

[a] Energy values are given in kcal/mol at BP86/TZ2P. [b] The values in parentheses are percentages and give the contribution to the total attractive interactions $\Delta E_{elstat} + \Delta E_{orb}$. [c] The values in parentheses are percentages and give the contribution to the orbital interaction ΔE_{orb}.

a σ- and a (weaker) π-donor. Figure 5 shows that the **1M** → CS_2 σ-donation in **2M** through the orbitals HOMO-3 and HOMO-6 comes mainly from the mixing of four occupied and two vacant orbitals, i.e., $7a_1-9a_1$ of CS_2 and $8a_1-10a_1$ of **1M**.

Orbitals g−j in Figure 4 give also the relevant occupied σ- and $\pi_{\perp}$-orbitals of **3M**. Visual inspection of the orbitals of the CO_2 complex **3M** indicate a similar carbon−carbon situation as for **2M**. The NBO calculations (Table 8) suggest a **1M** → CO_2 charge donation of 0.68 e in **3M** that is slightly higher than the **1M** → CS_2 charge donation in **2M**. The breakdown of the charge donation into orbitals having different symmetry shows that CO_2 is a weaker $\pi_{\perp}$-acceptor but a stronger σ-acceptor than CS_2. The **1M** → CO_2 $\pi_{\perp}$-donation is 0.07 e while the **1M** → CO_2 σ-donation in **3M** is 0.54 e. There is also **1M** → CO_2 $\pi_{\parallel}$-donation of 0.07 e (Table 8).

The orbital analysis of the molybdenum complex **5M** indicates two orbital contributions that are relevant for the metal−ligand interactions. They are shown in Figure 4k and l. The shape of the latter orbitals suggest that the HOMO-4 is a $(CO)_4Mo$ ← **2M** $\pi_{\parallel}$-donor orbital while the HOMO-6 is a $(CO)_4Mo$ ← **2M** σ-donor orbital. This is supported by calculated charges. The NBO calculations give an overall $(CO)_4Mo$ ← **2M** of 0.37 e. The contribution of the $\pi_{\parallel}$-orbitals is 0.24 e while the σ-orbitals donate 0.20 e. There is a small $(CO)_4M$ → **2M** $\pi_{\perp}$ back-donation of 0.07 e.

To get a more quantitative insight into the nature of the C−C and Mo−S interactions in **2**, **3**, and **5M** we carried out an energy decomposition analysis (EDA) as described in the Experimental Section. We also carried out EDA calculations of the model compounds **2M** and **3M** in order to compare the binding interactions with the bonding in the real systems. The EDA work was carried out using geometries that were optimized with C_{2v} symmetry constraint in order to distinguish between σ- and π-orbital interactions. Because of the very small energy differences it can be assumed that the nature of the bonding between the equilibrium structures and the C_{2v} forms is very similar. The results are shown in Table 9.

The EDA results suggest that the carbon−carbon bonding in **2** and **3** have more covalent than electrostatic character. The contributions of the ΔE_{orb} term to the total attractive interactions are 59.0% for **2** and 56.2% for **3**. The covalent bonding comes mainly from the a_1 (σ) orbitals, which contribute 82.3 (**2**) and 82.9% (**3**) of the total orbital interactions. The attractive interactions of the $\pi_{\perp}$-orbitals are much smaller. Only 10.4 (**2**) and 9.3% (**3**) of the ΔE_{orb} term come from the out-of-plane $\pi_{\perp}$-bond. The values for the relative energy contributions to the C−C bonding in **2M** and **3M** are very similar, which means that the model compounds may be used for analyzing the carbon−carbon bonds in the real systems. Note that the calculated C−C donor−acceptor bonds in **2M** and **3M** are slightly stronger than in **2** and **3**.

Is the weak $\pi_{\perp}$-bonding the reason for the nearly planar arrangement of the CS_2 and CO_2 ligands in **2** and **3,** which is strikingly different from the orthogonal structure of the CS_2 adduct of electron-rich carbenes?[5−7] We carried out an EDA analysis of the C−C bond of a model complex of the Arduengo carbene[42] 1,3-dimethylimidazol-2-ylidene with CS_2 (**2Ar**) (Figure 6). The geometry optimization of **2Ar** gave a structure where the CS_2 ligand is perpendicular to the carbene moiety which is in agreement with experiment. The geometry was also optimized with a coplanar arrangement of the ligand and carbene fragments (Figure 6). The EDA results for the planar structure of **2Ar**, which is 10.8 kcal/mol higher in energy than the equilibrium form, are given in Table 9. A comparison with the results for **2** shows that the $\pi_{\perp}$-bonding contributions in **2Ar** are indeed significantly weaker than in **2** and **2M**. The relative contributions in the former compound are only 21.4 kcal/mol (6.7%) while in the latter they are 40.0 (10.4%) (**2**) and 38.8 kcal/mol (8.6%) (**2**). The EDA results thus support the explanation of the nearly planar geometry of **2** in terms of stronger C−C $\pi_{\perp}$-bonding.

Table 9 gives also the EDA results for the C−C and Mo−S bonds of the molybdenum model complex **5M**. The former results shall be compared with the EDA data for **2M**. It becomes obvious that the nature of the C−C bond changes very little. We want to point out that the total attractive interactions in **5M** ($\Delta E_{int} = -96.8$ kcal/mol) are stronger than in **2M** ($\Delta E_{int} = -93.3$ kcal/mol) although the attractive components ΔE_{elstat} and ΔE_{orb} in the former compound are much weaker than in the latter (Table 9). The stronger net attraction comes from the significantly weaker Pauli repulsion in **5M** than in **2M**. This is because electronic charge is donated from the occupied orbitals of the CS_2 ligand toward molybdenum, which weakens the Pauli repulsion between the fragments CS_2 and **2M** in the complex **5M**.

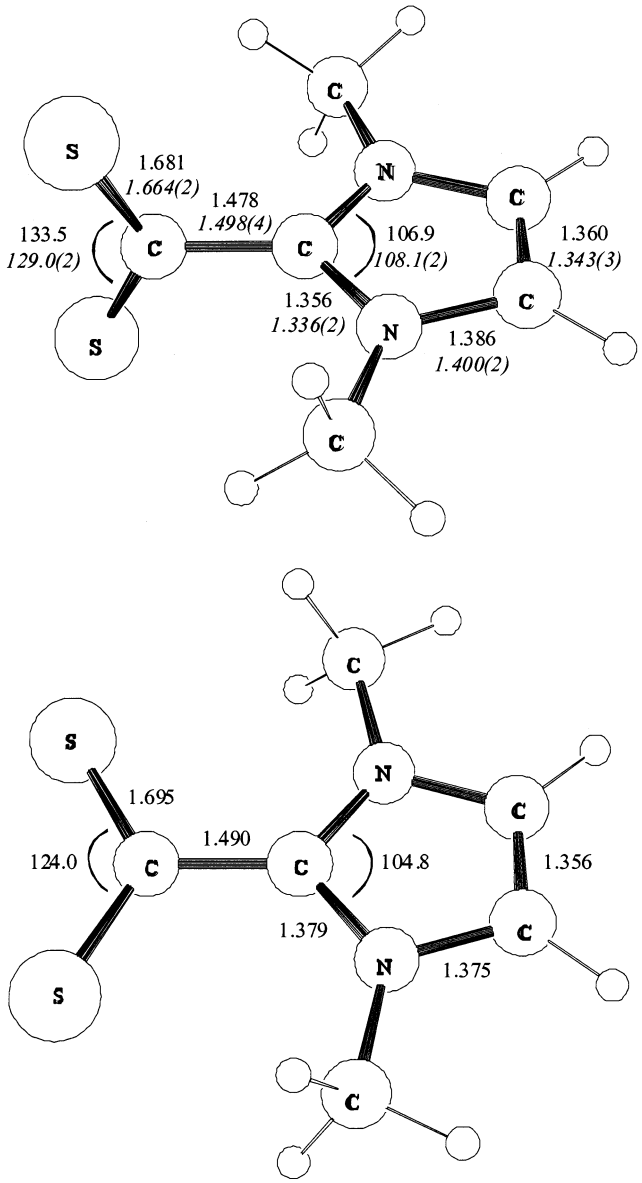

Figure 6. Optimized geometry at BP86/TZ2P of the Arduengo-type carbene complex with CS_2 as ligand **2Ar**. Top: Energy minimum structure. Bottom: Optimized geometry with enforced coplanar arrangement of the CS_2 ligand. Bond lengths are given in angstroms and angles in degrees. Experimental values are given in parentheses.

The EDA results for the Mo−S interactions in **5M** are very interesting. The data in Table 9 suggest that the $(CO)_4Mo$−**2M** interactions are slightly more electrostatic (54.6%) than covalent (45.4%). There are nearly equally strong contributions of the σ- (a_1) and $\pi_{\parallel}$-donor (b_2) orbitals, which dominate the ΔE_{orb} term. The latter contributions can easily be identified with the orbitals shown in structures k and l in Figure 4, which are the ± in-plane combinations of the sulfur lone-pair orbitals. The latter results demonstrate nicely the complementary nature of the charge and energy decomposition analyses, which give a coherent picture of the bonding interactions. It is an example of how the results of quantum chemical calculations can be used to build a bridge between qualitative chemical bonding models and accurate theoretical data.

Summary and Conclusions

The results of this work can be summarized as follows. The first X-ray structure analyses of the CS_2 and CO_2 adducts with carbodiphosphorane $C(PPh_3)_2$ show remarkably short carbon−carbon distances and a nearly planar arrangement of the CX_2 ligand and the CP_2 donor moiety. The CX_2 acceptor fragments in the complexes have acute X−C−X bonding angles of 124.8(3)° (CS_2) and 127.7(2)° (CO_2), which deviate significantly from the linear values of the free species. The X-ray structure analyses of group-6 carbonyl complexes $[(CO)_4MS_2CC(PPh_3)_2]$ (M = Cr, Mo, W) exhibit a distorted octahedron with small S−M−S angles of 67−70°. The charge and energy decomposition analysis show that carbodiphosphoranes $C(PR_3)_2$ are double electron pair donors having σ- and π-carbon lone-pair orbitals as the two highest occupied MOs. The NBO charge analysis of $(PH_3)_2C-CX_2$ indicates that $(PH_3)_2C$ is a σ- and π-donor. The energy decomposition analysis shows that the carbon−carbon bonding in $(PPh_3)_2C-CX_2$ and $(PH_3)_2C-CX_2$ comes from ~40% electrostatic attraction while ~60% of the attractive forces come from orbital interactions. The strongest orbital interactions come from the σ-orbitals, which contribute >80% to the ΔE_{orb} term. The molybdenum−sulfur bonding in $[(CO)_4MoS_2CC(PH_3)_2]$ has a slightly more electrostatic (54.6%) than covalent (45.4%) character. The bonding contributions of the orbital interactions come mainly from $[(CO)_4Mo \leftarrow S_2CC(PH_3)_2]$ σ-donation (40.8%) and $\pi_{\parallel}$-donation (42.3%).

Experimental Section

General Considerations. All operations were carried out under an argon atmosphere in dried and degassed solvents using Schlenk techniques. IR spectra (in Nujol) were run on a Nicolet 510 spectrometer. ^{31}P NMR spectra were run on a Bruker ARX 200 spectrometer and were referred to H_3PO_4 as external standard. Elemental analyses were performed by the analytical service of the Fachbereich Chemie der Universität Marburg (Germany). $C(PPh_3)_2$ (**1**), $S_2CC(PPh_3)_2$ (**2**), and $O_2CC(PPh_3)_2$ (**3**) were obtained according to a modified literature procedure,[10a] and commercially available $M(CO)_6$ were sublimed before use.

Preparation of $S_2CC(PPh_3)_2$ (2). To a solution of **1** in toluene was added an excess of CS_2. Immediately, a bright yellow orange precipitate was formed. The mixture was allowed to stand overnight, the residue was filtered and dried in a vacuum. IR (Nujol mull): 1480 m, 1437 s, 1262 w, 1181 m, 1159 m, 1142 s, 1099 s, 1067 s, 1026 m, 1001 m, 959 m, 930 w, 920 w, 851 w, 843 w, 793 w, 748 s, 741 s, 733 m, 718 m, 700 s, 692 s, 687 s, 619 w, 588 m, 561 m, 513 s, 492 s, 467 m, 449 m, 424 w, 411 m cm^{-1}.

Preparation of $O_2CC(PPh_3)_2$ (3). Through a solution of **1** in toluene was bubbled a stream of CO_2, which was dried over P_2O_5. A white precipitate formed, which was filtered and dried in a vacuum. IR (Nujol mull): 1582 s, 1566 s, 1480 m, 1437 m, 1295 s, 1185 w, 1162 m, 1147 s, 1104 s, 1070 m, 1028 w, 985 m, 788 w, 746 m, 714 m, 691 s, 536 m, 519 s, 504 s cm^{-1}.

Preparation of $[(CO)_4CrS_2CC(PPh_3)_2]$ (4). A THF solution of 0.44 g (2.00 mmol) of $Cr(CO)_6$ was irradiated for 6 h with a mercury lamp (TQ 150, 150 W). To the resulting orange solution of $Cr(CO)_5THF$ was added 1.05 g (1.72 mmol) of **2** and the mixture was stirred for 4 h at room temperature; filtration from small amounts of insoluble material gave a red solution. The ^{31}P NMR

spectrum showed the singlet of **4** and only traces of the byproducts $SPPh_3$ and SC_2PPh_3. On standing of the solution at 4 °C, red crystals of **4** separated and were dried in a vacuum. Yield: 0.64 g (0.70 mmol) 40.0%. ^{31}P NMR (THF): s, 8.9 ppm. IR (Nujol mull): 1989 s, 1864 vs, 1811 vs, all ν(CO), 1205 m, 1104 m, 1100 m, 1062 m, 999 w, 933 w, 817 w, 748 m, 720 w, 710 w, 685 m, 644 w, 523 m, 511 m cm^{-1}. Analyses: H 4.89 (5.03), C 63.26 (65.20)%.

Preparation of $[(CO)_4MoS_2CC(PPh_3)_2]$ (5). To a suspension of 0.42 g (0.70 mmol) of **2** in ~40 mL of THF was added 0.18 g (0.70 mmol) of $Mo(CO)_6$ and the mixture stirred for 4 d at room temperature. During the reaction time, the solution turned from colorless to orange. The solution was filtered from unreacted **2** (0.14 g) and concentrated to ~25 mL. The ^{31}P NMR of the solution exhibits three singlets. While the signals at 42.3 and 10.3 ppm belong to the decomposition products of **2**, $SPPh_3$ and SC_2PPh_3, respectively, the singlet at 14.7 ppm could be assigned to the complex **3**. The filtered solution was layered with pentane. After ~2 weeks orange red crystals separated, which were collected and dried in a vacuum. Yield: 0.12 g (0.12 mmol) 17%. The product could also be prepared according to the procedure described for the chromium derivative **4**; yield: 40−50%. ^{31}P NMR (THF): 14.7 ppm. IR (Nujol mull): 2000 s, 1987 sh, 1877 vs, 1851 vs, 1806 vs ν(CO), 1206 s, 1179 s, 1161 sh, 1098 s, 1067 s, 1053 m, 1026 w, 999 w, 808 m, 747 s, 720 m, 710 m, 690 s, 635 w, 594 w, 574.8 m, 557.5 m, 522,7 s, 509.2 m, 495.7 m cm^{-1}. Analyses: H 4.76 (4.81), C 63.47 (62.23)%.

Preparation of $[(CO)_4WS_2CC(PPh_3)_2]$ (6). The compound was prepared according to the procedure outlined for the chromium complex **4** starting with 0.53 g (1.50 mmol) of $W(CO)_6$ and 0.92 g (1.50 mmol) of **2**. The carbonyl was irradiated for 8 h at room temperature; yield: 0.58 g (0.6 mmol) 40%. Direct reaction of $W(CO)_6$ and **2** gave only small amounts of **6** as shown by NMR measurements; as the main products the decomposition products of **2**, $SPPh_3$ and S═C═C═PPh_3 were obtained. ^{31}P NMR (THF): 13.8 ppm. IR (Nujol mull): 1991 s, 1854 vs, 1813 vs, 1481 w, 1484 s, 1208 s, 1184 s, 1165 m, 1099 m, 1059 m, 1026 w, 999 w, 810 m, 750 m, 741 s, 719 w, 710 w, 573 w, 575 w, 522 s, 511 s, 494 m, 449 w cm^{-1}. Analyses: H 3.67 (3.63), C 52.07 (55.94)%.

Quantum Chemical Calculations. The geometries of the molecules have been optimized at the B3LYP[24] level using a scalar-relativistic small-core ECP with a (441/2111/31/1) valence basis set for Mo[26] and 6-311G(2d) basis sets[27] for the main-group elements where six d-type functions are used throughout. This is our basis set III.[28] The geometries were also optimized at B3LYP using the smaller basis set II, which has a scalar-relativistic small-core ECP with a (441/2111/31) valence basis set for Mo[26] and 6-31G(d) basis sets[27] for the main-group elements. The nature of the stationary points was examined by calculating the Hessian matrix at B3LYP/II. Bond energies have also been calculated at MP2/III[29] using B3LYP/III optimized geometries. The zero-point energy calculations were calculated at B3LYP/II. The atomic partial charges have been estimated with the NBO method of Weinhold.[30] The calculations have been carried out with the program packages Gaussian98 and Gaussian03.[31]

The nature of the donor−acceptor interactions has been analyzed with the energy decomposition scheme of the program ADF,[32,33] which is based on the energy partitioning methods suggested by Morokuma[34] and Ziegler.[35] To this end the geometries were optimized at BP86[25] in conjunction with uncontracted Slater-type orbitals (STOs) as basis functions.[36] The differences between the B3LYP/III and BP86/TZ2P optimized geometries are very small. Relativistic effects have been considered by the zero-order regular approximation (ZORA).[37] The basis set for Mo has triple-ζ quality augmented by two sets of 6p functions. Triple-ζ basis sets augmented by two sets of d-type polarization functions have been used for the main-group elements. This basis set is denoted TZ2P. The (1s2s2p3s3p)[18] core electrons of Mo were treated by the frozen-core approximation.[38a] An auxiliary set of s, p, d, f, and g STOs was used to fit the molecular densities and to represent the Coulomb and exchange potentials accurately in each SCF cycle.[38b]

For the energy decomposition analysis the interaction energy ΔE_{int} was calculated and decomposed for the bonding between the chosen donor and acceptor fragments. The instantaneous interaction energy ΔE_{int} can be divided into three components:

$$\Delta E_{int} = \Delta E_{elstat} + \Delta E_{Pauli} + \Delta E_{orb} \quad (2)$$

ΔE_{elstat} gives the electrostatic interaction energy between the fragments, which are calculated with a frozen electron density distribution in the geometry of the complex. It can be considered as an estimate of the *electrostatic* contribution to the bonding interactions. The second term in eq 2, ΔE_{Pauli}, gives the repulsive four-electron interactions between occupied orbitals. The last term gives the stabilizing orbital interactions ΔE_{orb}, which can be considered as an estimate of the *covalent* contributions to the bonding. Thus, the ratio $\Delta E_{elstat}/\Delta E_{orb}$ indicates the electrostatic/covalent character of the bond. The latter term can be partitioned further into contributions by the orbitals which belong to different irreducible representations of the point group of the interacting system. This makes it possible to calculate e.g. the contributions of σ- and π-bonding to a covalent multiple bond.[39] Technical details about the EDA method can be found in the literature.[33]

The BDE ΔE_e is given by the sum of ΔE_{int} and the fragment preparation energy ΔE_{prep}:

$$\Delta E_e = \Delta E_{prep} + \Delta E_{int} \quad (3)$$

ΔE_{prep} is the energy that is necessary to promote the fragments from their equilibrium geometry and electronic ground state to the geometry and electronic state they have in the optimized structure.

Acknowledgment. We are grateful to the Deutsche Forschungsgesellschaft and the Max-Planck-Society, Munich, Germany, for financial support.

Supporting Information Available: Additional information. This material is available free of charge via the Internet at http://pubs.acs.org.

IC048397L